AD-A258 041

TGAL-92-11

SIMULTANEOUS INVERSION OF EXPLOSION SIZE AND PATH ATTENUATION PARAMETER WITH CRUSTAL PHASES

Rong-Song Jih

Teledyne Geotech Alexandria Laboratory
314 Montgomery Street
Alexandria, Virginia 22314-1581

OCTOBER 1992

SEMI-ANNUAL REPORT: No. 2 (5 April 1992 - 23 October 1992)
ARPA ORDER NO.: 6731
PROJECT TITLE: Statistical Study of Soviet Explosion Magnitudes and Yields Using Heavily Censored Historical Yields, Soviet-released Analog Waveforms, and Digital Data Recorded at Modern Arrays
CONTRACT NO.: F29601-91-C-DB23

Prepared for:
UNITED STATES AIR FORCE
AIR FORCE SYSTEM COMMAND
PHILLIPS LABORATORY (PL)
KIRTLAND AFB, NM 87117-6008

Monitored by:
DEFENSE ADVANCED RESEARCH PROJECTS AGENCY
NUCLEAR MONITORING RESEARCH OFFICE
3701 NORTH FAIRFAX DRIVE
ARLINGTON, VA 22203-1714

REPORT DOCUMENTATION PAGE

Form Approved
OMB No. 0704-0188

1. AGENCY USE ONLY *(Leave blank)*

2. REPORT DATE
23 October 1992

3. REPORT TYPE AND DATES COVERED
Semi-annual Report, 5 April 1992 - 23 October 1992

4. TITLE AND SUBTITLE
Simultaneous Inversion of Explosion Size and Path Attenuation Parameters with Crustal Phase

5. FUNDING NUMBERS
Contract F29601-91-C-DB23

6. AUTHOR(S)
R.-S. Jih

7. PERFORMING ORGANIZATION NAME(S) AND ADDRESS(ES)
Teledyne Geotech
314 Montgomery Street
Alexandria, VA 22314-1581

8. PERFORMING ORGANIZATION REPORT NUMBER
TGAL-92-11

9. SPONSORING/MONITORING AGENCY NAME(S) AND ADDRESS(ES)
DARPA/NMRO (Attn. Dr. Alan Ryall)
3701 North Fairfax Drive
Arlington, VA 22203-1714

10. SPONSORING/MONITORING AGENCY REPORT NUMBER

11. SUPPLEMENTARY NOTES

12a. DISTRIBUTION/AVAILABILITY STATEMENT
Approved for Public Release; Distribution Unlimited

12b. DISTRIBUTION CODE

13. ABSTRACT *(Maximum 200 words)*

An iterative procedure is presented to invert for the path γ and the event $m_b(L_g)$ values simultaneously without using any *a priori* information about the path γ. This joint inversion scheme can be applied to data from multiple test sites as well. With this iterative method, it is rather easy to incorporate the appropriate boundary condition into the inversion. The iterative scheme is less sensitive to rounding errors, and hence it is numerically more accurate than those direct methods based on matrix factorization or Gaussian elimination. When the number of equations becomes large, the iterative method is often the only practical means to tackle the problem.

The iterative joint inversion scheme has been applied to Nuttli's Semipalatinsk $m_b(L_g)$ data set furnished by DARPA/NMRO. The result indicates that the majority of Q_0 values Nuttli used in his pioneering L_g study appear to be very good except for the path from Eastern Kazakh to COP (Copenhagen, Denmark). An 8% increase in Nuttli's postulated coefficient of anelastic attenuation, Q_0, for this particular path is necessary. Overall, Nuttli's (1986b, 1987) $m_b(L_g)$ data set for Semipalatinsk explosions appears to have very good quality with a standard deviation (of single observation) of only 0.1 magnitude unit.

14. SUBJECT TERMS
$m_b(L_g)$, Station Amplification, Anelastic Attenuation, General Linear Model, Iterative Method

15. NUMBER OF PAGES
42

16. PRICE CODE

17. SECURITY CLASSIFICATION OF REPORT	18. SECURITY CLASSIFICATION OF THIS PAGE	19. SECURITY CLASSIFICATION OF ABSTRACT	20. LIMITATION OF ABSTRACT
Unclassified	Unclassified	Unclassified	UL

(THIS PAGE INTENTIONALLY LEFT BLANK)

Table of Contents

List of Figures	iv
List of Tables	v
Summary	vii
1. Introduction	1
2. Joint Inversion Model	2
3. Iterative Inversion Procedure	4
4. Nuttli's Semipalatinsk $m_b(L_g)$ Data Set	7
5. Inversion Results with Nuttli's Data Set	13
6. Discussion and Conclusions	22
7. Acknowledgements	24
8. References	24
Distribution List	27

List of Figures

Figure No.	Caption	Page
1	The epicenters of all 89 Semipalatinsk underground nuclear explosions that Nuttli (1986b, 1987) studied. 57 events for which the individual station $m_b(L_g)$ values are available at DARPA/NMRO are shown in crosses, which include 31, 24, and 2 events from Balapan, Degelen Mountain, and Murzhik subsites, respectively. These 57 events covers most Degelen events (except the one on 12/03/75) as well as about half of the Balapan events used in Nuttli's (1986b, 1987) study. The 32 missing events are shown in diamonds.	8
2	The Q_0 values measured by Nuttli (1986b) with the coda-Q method (top), and those derived by the GLM scheme (bottom). The GLM joint inversion gives a Q_0 of 756 for the Kazakh-COP path, which is 8% higher than Nuttli's guess. Thus events solely recorded at the station COP (such as Balapan explosion 02/10/85) would have significant discrepancy between Nuttli's original $m_b(L_g)$ and the GLM/LSMF result. Nuttli did not have sufficient reliable data for the path from Eastern Kazakhstan to COP to determine the Q_0 and ζ with the coda-Q method, and hence the values for the station KON were used (Nuttli, 1986b; page 1243). The station COP is right on the same azimuth as Russian IRIS stations OBN for which Bennett *et al.* (1990) also find a Q_0 of 760.	16
3	The $m_b(L_g)$ station terms derived with LSMF inversion. Nuttli (1986b, 1987) already included the attenuation correction in his $m_b(L_g)$ determination, therefore the station residuals (inferred by LSMF) should be relatively small for $m_b(L_g)$. The large positive station term at COP would suggest that Nuttli could have underestimated the path Q_0 for all paths from Eastern Kazakh to COP. The bias of 0.180 can be translated to an increase of 8% in the path Q_0, which would yield a Q_0 estimate identical to what obtained with the GLM iterative inversion method.	17
4	GLM/LSMF-reprocessed $m_b(L_g)$ values versus Nuttli's (1986b, 1987) $m_b(L_g)$ values. The Balapan event 02/10/85 stands out as an outlier. For all other 56 events, Nuttli's event $m_b(L_g)$ values appear to be very consistent with our reprocessed results.	18

List of Tables

Table No.	Title	Page
1	Nuttli's station $m_b(L_g)$ of 57 Semipalatinsk explosions	9
2	Re-constructed station L_g amplitudes	11
3	GLM-inverted coefficient of anelastic attenuation versus LSMF-inferred station corrections	15
4	Comparison of various $m_b(L_g)$	19

(THIS PAGE INTENTIONALLY LEFT BLANK)

SUMMARY

This is our second semi-annual technical report prepared under DARPA contract **F29601-91-C-DB23**. It summarizes the research conducted during April - October, 1992. An iterative procedure is developed to invert for the path γ and the event $m_b(L_g)$ values simultaneously without using any *a priori* path γ information. This joint inversion scheme can be applied to data from multiple test sites as well. With this iterative method, it is rather easy to incorporate the appropriate boundary condition into the inversion. The iterative scheme is less sensitive to rounding errors, and hence it is numerically more accurate than those direct methods based on matrix factorization or Gaussian elimination. When the number of equations becomes large, the iterative method is often the only practical means to tackle the problem. The necessity of incorporating an extra boundary condition is also reviewed in this report. This joint inversion scheme is a natural extension to crustal phases of the one we used in the m_b analyses (*cf.* our first semi-annual technical report *TGAL-92-05).*

The joint inversion scheme has been applied to Nuttli's Semipalatinsk $m_b(L_g)$ data set recovered by DARPA/NMRO. The result indicates that the majority of Q_0 values Nuttli used in his pioneering L_g study are very good except for the path from Eastern Kazakh to COP (Copenhagen, Denmark). An 8% increase in Nuttli's postulated coefficient of anelastic attenuation, Q_0, for this particular path is necessary. Overall, Nuttli's (1986b, 1987) $m_b(L_g)$ data set for Semipalatinsk explosions appears to have very good quality with a standard deviation (of single observation) of only 0.1 magnitude unit.

(THIS PAGE INTENTIONALLY LEFT BLANK)

1. INTRODUCTION

The standard procedure used in estimating the source size of underground nuclear explosions using m_b measurements has been to separate the station terms from the network-averaged source terms. The station terms thus derived actually reflect the combination of the path effect and the station effect, when only those events in a close proximity are utilized. If worldwide explosions are used in the inversion, then the path effect tends to be averaged out at each station. In either case, the effect due to the propagation path alone would not be obvious. Recently Jih and Wagner (1991, 1992ab) decomposed the station m_b with the following joint model:

$$E(i) + S(j) + F(k(i),j) + \varepsilon(i,j) = \log_{10}[A(i,j)/T(i,j)] + B(\Delta(i,j)) \ . \qquad [1]$$

The right-hand side of [1] is the conventional raw station m_b of the i-th event (of "true" size E(i)) observed at the j-th station where A, T, and B(Δ) are the displacement amplitude, the dominant period, and the distance-correction term, respectively. On the left-hand side, S represents the station correction, and F(k(i),j) is the path correction at the j-th station for explosions from the k(i)-th source region. Applying this joint inversion model yields a reduction in the fluctuational variation of station m_b by a factor ranging from 1.2 to 3.0 (Jih and Wagner, 1992ab).

Underground nuclear explosions at continental test sites produce crustal phases that can be observed at near or regional distances, of which the most prominent often is L_g. It is natural to ask if the joint inversion scheme described in Equation [1] can be extended to L_g. In this study, an iterative procedure is presented to invert for the path γ and the event $m_b(L_g)$ values simultaneously without the need to measure the path γ with other methods in advance. This joint inversion scheme can be applied to data from multiple test sites as well. With this iterative method, it is rather easy to incorporate the boundary condition into the inversion. The iterative scheme is less sensitive to rounding errors, and hence it is numerically more accurate than those direct methods based on matrix factorization or row elimination. When the number of equations becomes huge, the iterative method is often the only practical means to tackle the problem. The need of incorporating extra boundary conditions in this type of inversion problem is also reviewed.

The iterative joint inversion scheme has been tested with Nuttli's Semipalatinsk $m_b(L_g)$ data set furnished by DARPA/NMRO. The result indicates that the majority of Q_0 values Nuttli used in his pioneering L_g study are very good except for the path from Eastern Kazakh to COP (Copenhagen, Denmark). An 8% increase in Nuttli's postulated coefficient of anelastic

attenuation for this particular path is necessary. Overall, Nuttli's (1986b, 1987) $m_b(L_g)$ data for Semipalatinsk explosions appear to have very good quality with a standard deviation (of single observation) of 0.1 magnitude unit [m.u.].

2. JOINT INVERSION MODEL

For the purpose of calculating the individual $m_b(L_g)$, Nuttli's (1986ab) original formulae can be rewritten in a slightly more convenient form (Jih and Lynnes, 1992):

$$m_b(L_g) \equiv 4.0272 + \log A(\Delta) + \frac{1}{3}\log(\Delta) + \frac{1}{2}\log[\sin(\frac{\Delta(\mathrm{km})}{111.1(\mathrm{km/deg})})] + \frac{\gamma(\Delta - 10\mathrm{km})}{\ln(10)} , \qquad [2]$$

$$\text{where } \gamma \equiv \frac{\pi}{Q \cdot U \cdot T} , \qquad Q(f) = Q_0 \cdot f^{\zeta} ,$$

Δ is the epicentral distance in kilometers, $A(\Delta)$ is the observed 0-to-peak L_g amplitude measured in the time domain in microns [μm] at the epicentral distance of Δ km. The term $\frac{1}{3}\log(\Delta)$ accounts for the dispersion when measurements are made in the time domain. The terms $0.5 \cdot \log[\sin(\Delta(\mathrm{km})/111.1(\mathrm{km/deg}))]$ and $\gamma(\Delta - 10\mathrm{km})/\ln(10)$ correct for the geometrical spreading and the anelastic attenuation, respectively, where γ is the coefficient of anelastic attenuation. For instance, a seismic source with 1-sec L_g amplitude of 110 μm at 10-km epicentral distance would correspond to a $m_b(L_g)$ of 4.0272 + 2.0414 + 0.3333 - 1.4019 + 0.0000 = 5.000, same as what Nuttli's original formulae would give. This formula is appropriate for events in eastern North America and Central Asia.

Now consider the case of m explosions recorded at some or all of n stations. For simplicity, we assume that these m explosions are detonated in the same test site for the moment. The case of multiple test sites will be discussed later. The linear model for L_g phases can then be written as

$$E(i) - \gamma(j)(\Delta(i,j) - 10\mathrm{km})/\ln(10) + \varepsilon(i,j) = Y(i,j) , \qquad [3]$$

$$\text{where } Y(i,j) \equiv 4.0272 + \log A(i,j) + \frac{1}{3}\log(\Delta(i,j)) + \frac{1}{2}\log[\sin(\frac{\Delta(i,j)}{111.1(\mathrm{km/deg})})] .$$

Once the amplitudes and the locations of the events (and hence the epicentral distances, Δ) are available, Y would be completely known. Only the event sizes (E) and the path-specific coefficients of anelastic attenuation (γ) are the unknown parameters to be determined. The obscuring errors ε are assumed to be uncorrelated and to belong to the same probability distribution, namely a common Gaussian distribution with zero mean and variance σ^2. Our

model (Equation [3]) is a special case of a more general linear system:

$$E(i) + S(j) + \varepsilon(i,j) = Y(i,j)\ , \quad \text{for } i = 1,\dots,m\ ;\ j = 1,\dots,n\ . \tag{4}$$

which can be expressed in a matrix formulation:

$$\mathbf{H}\,X + \mathbf{e} = Y\ , \tag{5}$$

where **H** is the design (or observation) matrix. X and Y are the column vectors of unknowns and observations, respectively. The standard least-squares (LS) solution (*viz.*, the one that minimizes the *residual sum of squares:* RSS $\equiv (Y - \mathbf{H}\hat{X})'\,(Y - \mathbf{H}\hat{X})$) to *any* linear system with a general form like Equation [5] is

$$\hat{X}_{LS} \equiv (\mathbf{H}'\mathbf{H})^{-1}\mathbf{H}'Y\ , \tag{6}$$

where **H′** is the transpose of **H**. This least-squares estimator has many optimality properties. For instance, it is unbiased, and it gives minimum variance within the class of linear unbiased estimators. Furthermore, $\hat{X}_{LS}$ is also the *Maximum-Likelihood Estimate* (MLE) under the Gaussian assumption. It is straightforward to compute the uncertainty by using Var[$\hat{X}_{LS}$] ≡ the diagonal of $\sigma^2(\mathbf{H}'\mathbf{H})^{-1}$, which is simply scaling the variance of the random perturbations by the number of observations associated with each unknown.

In our case, however, the matrix **H′H** in Equation [6] is singular, and hence the least-squares theory can not be applied immediately unless the linear system of [4] is modified somewhat. Perhaps the easiest way to illustrate the indeterminacy due to the singularity of the matrix **H′H** is that given any set of solution to [4], we can always obtain yet another set of solution by adding a constant to all event magnitudes, E(i), i = 1,..., m, and subtracting the same constant from each station term S(j) (Jih and Shumway, 1989). Alternatively, we can verify that the matrix **H′H** has zero determinant with linear algebra packages such as LINPACK, EISPACK, or LAPACK. In this study, however, a formal proof is presented below. Without loss of generality, we can assume that each of the m events is fully recorded at all n stations, then

$$X \equiv [E_1, E_2, E_3, \dots, E_m, S_1, S_2, \dots, S_n]'\ , \quad \mathbf{H}'\mathbf{H} = \begin{bmatrix} n\cdot I_m & 1_{m\times n} \\ 1_{n\times m} & m\cdot I_n \end{bmatrix}$$

where I_m is the identity matrix of order m, and all elements of the m-by-n matrix $1_{m\times n}$ are 1. For instance, if m = 3 and n = 2, then

$$\mathbf{H'H} = \begin{bmatrix} 2 & 0 & 0 & 1 & 1 \\ 0 & 2 & 0 & 1 & 1 \\ 0 & 0 & 2 & 1 & 1 \\ 1 & 1 & 1 & 3 & 0 \\ 1 & 1 & 1 & 0 & 3 \end{bmatrix}$$

which is a *doubly-bordered band diagonal* sparse matrix (Tewarson, 1973; Press *et al.*, 1988). After exactly n row operations eliminating the lower-left submatrix, 1_{nxm}, the determinant of **H'H** can be computed (up to a multiplicative constant) as that of

$$\begin{bmatrix} I_m & (\frac{1}{n})_{nxm} \\ 0_{nxm} & P_n \end{bmatrix} \qquad [7]$$

where P_n is a square matrix of order n with $\frac{-m}{n}(n-1)$ on the diagonal and $\frac{-m}{n}$ elsewhere. For m = 3 and n = 2, [7] becomes

$$\begin{bmatrix} 1 & 0 & 0 & 0.5 & 0.5 \\ 0 & 1 & 0 & 0.5 & 0.5 \\ 0 & 0 & 1 & 0.5 & 0.5 \\ 0 & 0 & 0 & 1.5 & -1.5 \\ 0 & 0 & 0 & -1.5 & 1.5 \end{bmatrix}$$

It suffices to examine the determinant of this P_n, or, equivalently, to check the determinant of a square matrix of order n with n-1 on the diagonal and -1 elsewhere:

$$\begin{bmatrix} n-1 & -1 & -1 & \cdots & -1 \\ -1 & n-1 & -1 & \cdots & -1 \\ -1 & -1 & n-1 & \cdots & -1 \\ \cdots & \cdots & \cdots & \cdots & \cdots \\ -1 & -1 & -1 & \cdots & n-1 \end{bmatrix}$$

It is straightforward to prove that, by *mathematical induction,* this matrix has zero determinant for any n ≥ 2. Thus the matrix **H'H** in our linear model is always singular regardless how good the observed amplitudes/magnitudes, Y, might be. We therefore need an extra boundary condition to constrain our linear model for a unique solution. The most commonly adopted approach in teleseismic magnitude determination is to have all station terms sum up to zero (Douglas, 1966; Blandford and Shumway, 1982; Jih and Shumway, 1989; Murphy *et al.*, 1989; Jih and Wagner, 1992ab; and many others). This implies that larger events would tend to be unchanged whether we apply the station corrections or not, and hence the bulletin magnitudes of larger events published by ISC and NEIC can be regarded as more or less unbiased. This boundary condition can be incorporated into [4] by replacing all S(n) by $-\sum_{i=1}^{n-1} S(i)$. It not only reduces the number of unknowns by one, but, more importantly, regularizes the whole linear system to make **H'H** invertible. However, this is not the only boundary condition feasible. We can impose the extra constraint on E(i) instead, or, even impose the

constraint on *some* selected stations.

3. ITERATIVE INVERSION PROCEDURE

Once an extra boundary condition has been chose~, the inverse matrix of **H'H** in Equation [6] can be computed with matrix factorization (such as *Singular Value Decomposition,* [SVD]) or *Gaussian elimination* method. Numerical algorithms of these types are called *direct methods.* Direct methods can be impractical if **H'H** is large and sparse. The linear system solved in Jih and Wagner (1992ab) for the optimal m_b estimates involved 2733 unknown parameters and 24529 amplitude measurements. For these types of problems, iterative methods are often the only possible method of solution, as well as being faster and more accurate than Gaussian elimination and matrix factorization in many cases. The largest area for the application of iterative methods is that of the linear systems arising in the numerical solution of partial differential equations. Systems of orders 10,000 to 100,000 are not unusual in aerospace sciences, although the majority of the coefficients of the systems are typically zeros.

The basic idea of iterative methods is that one starts with a trial solution vector $X^{(0)}$ and carries out some process using **H**, Y, and $X^{(0)}$ to get a new vector $X^{(1)}$. Then one repeats. At the k stage, one uses the iterative process to get $X^{(k)}$ from **H** (or **H'H**), Y, and $X^{(k-1)}$. The specific algorithm for our problem is summarized in five steps:

Step 0

Set initial value of $\gamma(j)$ for j = 1,..., n.

Step 1

Compute event $m_b(L_g)$, E(i), for i = 1,..., m:

$$E(i) = \frac{1}{\#(j)}\sum_j[Y(i,j) + \gamma(j)[\Delta(i,j)-10\text{km}]/\ln(10)] ,$$

where #(j) is the number of stations used in the summation.

Step 2

Adjust E(i), i = 1,..., m, with the desired boundary condition.

Step 3

Compute the path-specific coefficient of anelastic attenuation, $\gamma(j)$, for j=1,..., n:

$$\gamma(j) = \ln(10)\sum_i[\ E(i) - Y(i,j)\ ]/\sum_i[\Delta(i,j)-10\text{km}] .$$

Step 4

Fill in missing paths (i,j) with predicted pseudo-observations:

$$Y(i,j) \equiv E(i) + \gamma(j)(\Delta(i,j) - 10km)/\ln(10)\ .$$

Step 5

Repeat steps [1]-[4] to update E and γ till convergence.

Although an arbitrary guess of γ will do at Step 0, picking an initial γ close to the average across the whole area of interest would speed up the convergence. The choice of the extra boundary condition (at Step 2) is very flexible. Constraining the mean of all event $m_b(L_g)$ seems to perform extraordinarily well, however. Note that the pseudo-observations predicted at Step 4 are treated as "good" observations at steps 1 and 3 except during the first iteration loop.

The iterative procedure described above is a special case of a general algorithm known variously as the *Gaussian-Seidel* method, the *Liebmann process,* or the *method of successive displacements* (Bunch and Rose, 1976; Forsythe *et al.*, 1977; Golub and Van Loan, 1983; Spedicato, 1991). The major difference between this method and that of *Gaussian-Jacobi (viz.,* the *simultaneous displacement* method) is that we solve for one component (*viz.*, E(i) or $\gamma(j)$) *of the new vector* X *using for each other component of* X *its most recently computed* value, whereas Gaussian-Jacobi method updates all unknown parameters simultaneously at the end of each iteration loop. *In our case,* Gaussian-Seidel method converges faster than does Gaussian-Jacobi method.

The advantage of our multi-event joint inversion scheme, as compared to the simple network averaging for each individual event that Nuttli (1986ab, 1987, 1988) used, is that we can have a more consistent network for all events. By "consistent" it means that the joint inversion procedure provides the best approximation to the network-averaged values that would have been obtained if all the events were recorded at every station in the network (Murphy *et al.*, 1989). This advantage may not be very obvious in using direct methods such as SVD or Gaussian elimination. However, it would become quite natural as revealed by Step 4 of our iteration scheme.

4. NUTTLI'S SEMIPALATINSK $m_b(L_g)$ DATA SET

Figure 1 shows the epicenters of all Semipalatinsk underground nuclear explosions that Nuttli (1986b, 1987) studied. The epicenters used in this study (for computing the epicentral distance, Δ) are those of Lilwall and Farthing (1990). 57 events for which the individual station $m_b(L_g)$ values are available at DARPA/NMRO are listed in Table 1. The events are sorted and identified by their dates (year, month, and day) and the subregion they are located. There are 31, 24, and 2 events from Balapan, Degelen Mountain, and Murzhik subsites, respectively (shown in crosses in Figure 1). These 57 events cover most Degelen events (except the one on 12/03/75) as well as about half of the Balapan events that were used in Nuttli's (1986b, 1987) study. The average of these 57 event magnitudes is 5.535. This value will be used to constrain our event $m_b(L_g)$ estimates so that the new magnitudes would be in alignment with those of Nuttli's (1986b, 1987). Semipalatinsk test range has long been divided into three test sites geographically, namely, Balapan, Degelen, and Murzhik. It has also been suggested by several recent yield estimation studies (*e.g.*, Marshall *et al.*, 1984; Ringdal *et al.*, 1992; Jih and Wagner, 1992ab) to further partition Balapan test site into three smaller subregions for better results based on m_b measurements. In this study, however, no attempt is made to separate the explosions according to their source media. All explosions are assumed to belong to the same test site, and they share the same propagation effect to any single recording station.

To our best knowledge, Nuttli's original amplitude measurements are no longer available. To test our new joint inversion scheme (Equation [3]), these 157 $m_b(L_g)$ magnitudes are converted to the theoretical ground displacement in nanometers [nm] of Airy phase, assuming a constant group velocity of 3.5 km/sec and a period of 1 second using the following formula:

$$A(\Delta) \equiv 10^{m_b(L_g)-4.0272} \cdot \Delta^{-0.333} \cdot [\sin(\Delta/111.1)]^{-0.5} \cdot \exp^{-\gamma(\Delta-10km)}, \qquad [9]$$

Nuttli's (1986b) path Q_0 values (*cf.* Table 5) are used in [9] to determine the path γ, and the re-constructed station amplitudes are listed in Table 2. Note that Nuttli (1986b) estimated the Q_0 and ζ with the coda-Q method for 10 out of 11 WWSSN stations, and he assumed that the station COP (Copenhagen, Denmark) has the same Q_0 of 700 as that of the station KON (Konsberg, Norway).

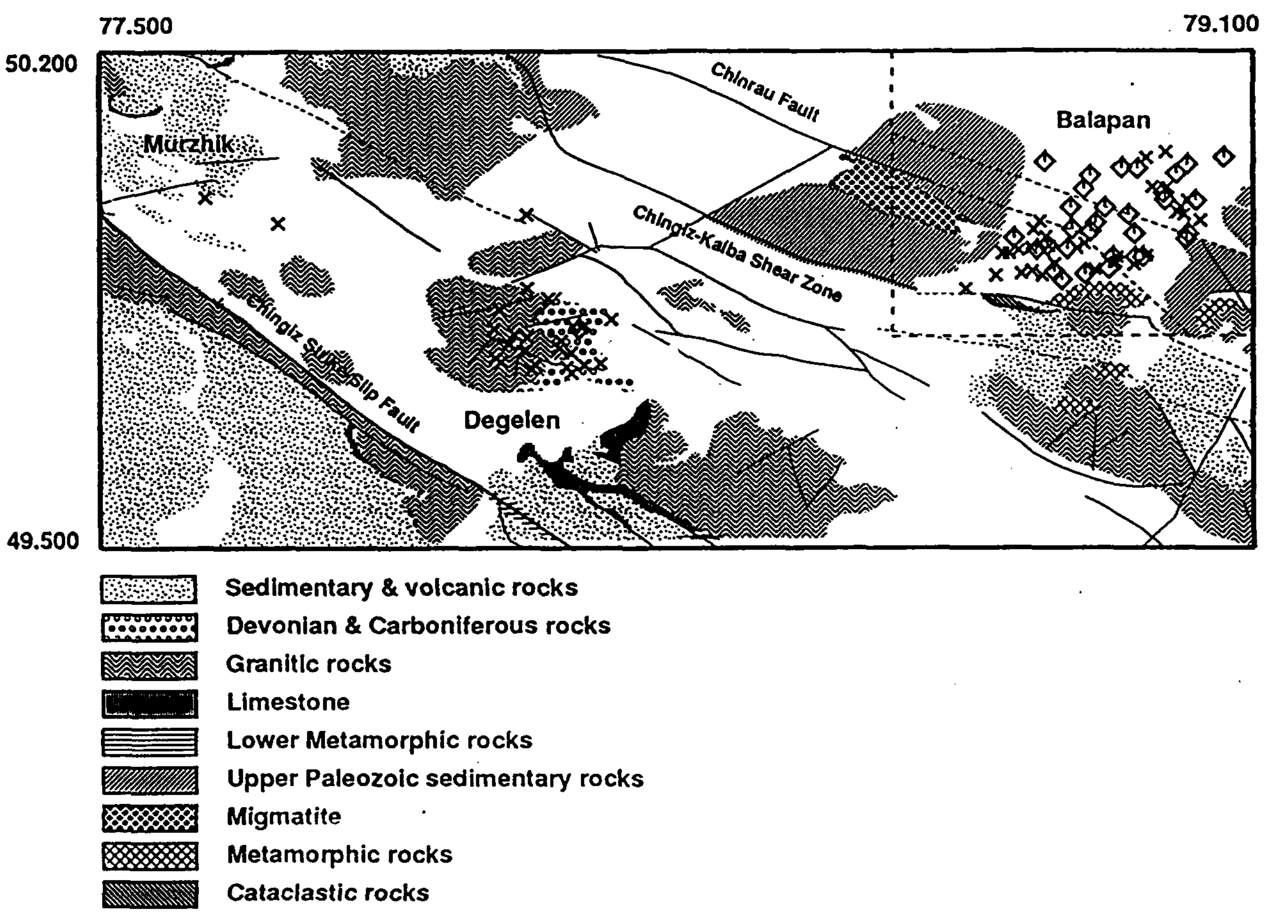

Figure 1. The epicenters of all 89 Semipalatinsk underground nuclear explosions that Nuttli (1986b, 1987) studied. 57 events for which the individual station $m_b(L_g)$ values are available at DARPA/NMRO are shown in crosses, which include 31, 24, and 2 events from Balapan, Degelen Mountain, and Murzhik subsites, respectively. These 57 events covers most Degelen events (except the one on 12/03/75) as well as about half of the Balapan events used in Nuttli's (1986b, 1987) study. The 32 missing events are shown in diamonds.

Table 1. Nuttli's Station $m_b(L_g)$ of 31 Balapan Explosions Furnished by NMRO													
Event *	N	Mean	KBL	MHI	NDI	NIL	QUE	SHL	COP	KON	KEV	NUR	UME
761123B	3	5.857	5.76	—	5.95	—	—	5.86	—	—	—	—	—
781129B	4	6.007	—	—	6.09	6.01	5.98	5.95	—	—	—	—	—
791028B	5	6.062	—	—	6.02	—	—	6.09	—	6.08	—	6.07	6.05
791202B	2	6.050	—	—	—	—	—	—	—	6.02	—	6.08	—
791223B	6	6.120	—	—	6.15	—	6.10	6.16	—	6.05	—	6.15	6.11
800612B	5	5.742	5.90	—	5.75	5.55	5.70	—	—	—	—	5.81	—
800629B	5	5.708	5.55	—	—	5.75	5.85	—	—	—	—	5.52	5.87
801012B	5	5.918	—	—	5.89	—	6.04	—	—	5.88	5.83	5.95	—
801214B	4	5.932	—	—	—	—	—	5.94	—	—	5.87	5.89	6.03
801227B	7	5.996	—	—	5.99	—	5.96	6.06	6.10	—	6.04	5.79	6.03
810329B	2	5.450	5.55	—	—	5.35	—	—	—	—	—	—	—
810422B	4	5.968	—	—	—	5.90	5.96	—	—	—	—	5.99	6.02
810913B	6	6.098	—	—	6.29	—	—	6.28	—	6.12	5.95	5.94	6.01
811018B	5	6.088	—	—	5.93	—	—	6.23	—	6.26	6.02	6.00	—
811227B	5	6.146	—	—	6.39	—	—	6.11	—	6.17	6.02	6.04	—
820425B	7	6.126	—	—	6.30	—	—	6.19	6.22	6.14	5.86	6.17	6.00
820704B	2	6.135	—	—	—	—	—	—	6.15	6.12	—	—	—
821205B	2	6.210	—	—	—	—	—	6.30	—	—	—	6.12	—
831006B	2	5.930	—	—	—	—	—	—	—	—	5.86	6.00	—
831026B	1	6.100	—	—	—	—	—	—	—	—	—	6.10	—
840219B	1	5.740	—	—	—	—	—	—	—	—	—	5.74	—
840307B	1	5.680	—	—	—	—	—	—	—	—	—	5.68	—
840329B	1	5.970	—	—	—	—	—	—	—	—	—	5.97	—
840425B	2	5.860	—	—	—	—	—	—	5.85	—	—	5.87	—
840526B	2	6.065	—	—	—	—	—	—	—	—	6.02	6.11	—
840714B	3	6.170	—	—	—	—	—	—	6.52	—	5.80	6.19	—
841027B	2	6.095	—	—	—	—	—	—	—	—	6.04	6.15	—
841202B	1	5.970	—	—	—	—	—	—	—	—	—	5.97	—
841216B	1	6.080	—	—	—	—	—	—	—	—	—	6.08	—
841228B	2	6.130	—	—	—	—	—	—	6.26	—	—	6.00	—
850210B	1	5.980	—	—	—	—	—	—	5.98	—	—	—	—

*: year, month, date, and site (B: Balapan; D: Degelen; M: Murzhik).

Table 1. Nuttli's Station $m_b(L_g)$ of 24 Degelen and 2 Murzhik Furnished by NMRO													
Event			Station										
Date	N	Mean	KBL	MHI	NDI	NIL	QUE	SHL	COP	KON	KEV	NUR	UME
730710D	2	5.070	5.00	—	—	5.14	—	—	—	—	—	—	—
731026D	1	4.910	—	—	—	4.91	—	—	—	—	—	—	—
740130D	2	5.125	5.05	—	—	5.20	—	—	—	—	—	—	—
740516D	2	4.860	4.86	—	—	4.86	—	—	—	—	—	—	—
740710D	2	4.780	4.87	—	—	4.69	—	—	—	—	—	—	—
740913D	1	4.810	—	—	—	4.81	—	—	—	—	—	—	—
741216aD	2	4.530	4.55	—	—	4.51	—	—	—	—	—	—	—
741216bD	2	4.430	4.38	—	—	4.48	—	—	—	—	—	—	—
750220D	3	5.410	5.50	—	5.43	5.30	—	—	—	—	—	—	—
750311D	2	5.315	—	5.37	—	5.26	—	—	—	—	—	—	—
760421aD	1	5.100	—	—	5.10	—	—	—	—	—	—	—	—
750608D	2	5.120	5.24	—	—	5.00	—	—	—	—	—	—	—
750807D	2	4.940	4.95	—	—	4.93	—	—	—	—	—	—	—
760115D	2	4.960	—	—	4.94	—	—	—	—	—	—	4.98	—
760723D	1	4.640	4.64	—	—	—	—	—	—	—	—	—	—
761230D	1	4.800	—	4.80	—	—	—	—	—	—	—	—	—
770329D	4	5.335	—	5.33	—	5.38	—	5.29	—	—	—	5.34	—
770425D	2	4.975	—	4.89	5.06	—	—	—	—	—	—	—	—
770730D	3	4.763	4.66	4.79	—	—	—	—	—	—	—	4.84	—
771226D	1	4.590	—	4.59	—	—	—	—	—	—	—	—	—
780326D	5	5.436	—	5.42	5.38	5.29	—	5.70	—	—	—	5.39	—
780422D	4	5.080	—	4.84	5.05	—	—	5.23	—	—	—	5.20	—
780728D	3	5.330	—	5.33	—	—	—	—	—	—	—	5.37	5.29
781129D	4	5.740	—	—	5.62	—	—	5.79	—	—	—	5.83	5.72
730419M	2	5.080	—	—	—	5.06	—	—	—	—	—	5.10	—
780319M	2	5.000	—	5.05	—	4.95	—	—	—	—	—	—	—

Table 2. Re-constructed Station L_g Amplitudes											
Event	Station 0-to-peak L_g Amplitude (nm) Predicted at 1 Hz										
Date	KBL	MHI	NDI	NIL	QUE	SHL	COP	KON	KEV	NUR	UME
761123B	72.4	—	8.9	—	—	3.2	—	—	—	—	—
781129B	—	—	12.5	180.5	8.4	3.9	—	—	—	—	—
791028B	—	—	10.5	—	—	5.5	—	32.1	—	42.5	41.4
791202B	—	—	—	—	—	—	—	28.1	—	43.9	—
791223B	—	—	14.6	—	11.2	6.4	—	30.3	—	51.9	48.2
800612B	100.3	—	5.6	61.3	4.3	—	—	—	—	23.4	—
800629B	46.2	—	—	99.4	6.2	—	—	—	—	12.1	27.7
801012B	—	—	7.8	—	9.3	—	—	20.2	26.8	32.1	—
801214B	—	—	—	—	—	3.9	—	—	29.3	28.0	39.4
801227B	—	—	9.5	—	7.6	5.0	34.7	—	44.3	22.6	40.1
810329B	44.5	—	—	38.4	—	—	—	—	—	—	—
810422B	—	—	—	142.7	8.2	—	—	—	—	35.6	38.8
810913B	—	—	20.1	—	—	8.6	—	35.2	35.3	31.5	37.7
811018B	—	—	8.7	—	—	7.6	—	48.8	41.7	36.4	—
811227B	—	—	25.2	—	—	5.7	—	39.9	41.9	40.2	—
820425B	—	—	20.6	—	—	7.0	45.4	36.8	28.7	53.4	36.8
820704B	—	—	—	—	—	—	39.2	35.6	—	—	—
821205B	—	—	—	—	—	8.9	—	—	—	48.2	—
831006B	—	—	—	—	—	—	—	—	29.0	36.7	—
831026B	—	—	—	—	—	—	—	—	—	45.9	—
840219B	—	—	—	—	—	—	—	—	—	20.1	—
840307B	—	—	—	—	—	—	—	—	—	17.6	—
840329B	—	—	—	—	—	—	—	—	—	33.6	—
840425B	—	—	—	—	—	—	19.5	—	—	27.0	—
840526B	—	—	—	—	—	—	—	—	41.6	46.5	—
840714B	—	—	—	—	—	—	90.6	—	25.0	56.1	—
841027B	—	—	—	—	—	—	—	—	43.9	51.8	—
841202B	—	—	—	—	—	—	—	—	—	33.8	—
841216B	—	—	—	—	—	—	—	—	—	44.0	—
841228B	—	—	—	—	—	—	50.5	—	—	36.7	—
850210B	—	—	—	—	—	—	26.4	—	—	—	—

Table 2. Re-constructed Station L_g Amplitudes											
Event	Station 0-to-peak L_g Amplitude (nm) Predicted at 1 Hz										
Date	KBL	MHI	NDI	NIL	QUE	SHL	COP	KON	KEV	NUR	UME
730710D	14.6	—	—	26.5	—	—	—	—	—	—	—
731026D	—	—	—	15.7	—	—	—	—	—	—	—
740130D	16.2	—	—	30.1	—	—	—	—	—	—	—
740516D	10.7	—	—	14.1	—	—	—	—	—	—	—
740710D	10.8	—	—	9.4	—	—	—	—	—	—	—
740913D	—	—	—	12.5	—	—	—	—	—	—	—
741216aD	5.2	—	—	6.2	—	—	—	—	—	—	—
741216bD	3.4	—	—	5.7	—	—	—	—	—	—	—
750220D	46.3	—	2.9	38.4	—	—	—	—	—	—	—
750311D	—	20.5	—	35.3	—	—	—	—	—	—	—
760421aD	—	—	1.4	—	—	—	—	—	—	—	—
750608D	25.7	—	—	19.4	—	—	—	—	—	—	—
750807D	12.8	—	—	16.2	—	—	—	—	—	—	—
760115D	—	—	0.9	—	—	—	—	—	—	3.7	—
760723D	6.4	—	—	—	—	—	—	—	—	—	—
761230D	—	5.5	—	—	—	—	—	—	—	—	—
770329D	—	18.1	—	43.7	—	0.8	—	—	—	8.6	—
770425D	—	6.7	1.2	—	—	—	—	—	—	—	—
770730D	6.7	5.4	—	—	—	—	—	—	—	2.7	—
771226D	—	3.3	—	—	—	—	—	—	—	—	—
780326D	—	23.2	2.6	37.8	—	2.2	—	—	—	9.5	—
780422D	—	6.0	1.2	—	—	0.7	—	—	—	6.0	—
780728D	—	18.7	—	—	—	—	—	—	—	9.0	7.5
781129D	—	—	4.5	—	—	2.6	—	—	—	26.3	20.5
730419M	—	—	—	21.2	—	—	—	—	—	5.2	—
780319M	—	10.0	—	16.5	—	—	—	—	—	—	—

5. INVERSION RESULTS WITH NUTTLI'S DATA SET

We carried out experiments to test two different inversion schemes. In the first test, the re-constructed station L_g amplitudes (Table 2) are fed into the iterative inversion procedure, with a boundary condition that 57 events would have a mean $m_b(L_g)$ of 5.535. In the second experiment, we fed the 157 station $m_b(L_g)$ values in Table 1 into a standard LSMF [Least Squares Matrix Factorization] (Douglas, 1966) inversion package based on SVD, with a boundary condition that ten stations (excluding COP) maintain an average station bias of zero. For convenience, these two experiments are denoted as "GLM" [General Linear Model] and "LSMF", respectively, in our discussion.

Note that Nuttli's station $m_b(L_g)$ values have already been corrected for the anelastic attenuation. If all the Q_0 values Nuttli (1986ab) applied are appropriate, then his station L_g magnitudes should be very consistent. As a result, the station bias should all be negligibly small if a LSMF-type inversion is applied. Conversely, if a prominent station correction is still present, then this would mean that the original attenuation correction Nuttli used may not be quite appropriate for certain paths. In other words, our LSMF station terms will give a direct clue of any un-accounted path effect such as that due to inaccurate attenuation correction.

The GLM inversion scheme, on the other hand, utilizes the raw amplitude measurements and inverts for both the event magnitudes and the coefficients of path attenuation simultaneously. We can then compare the resulting path Q_0 values with those obtained with the coda-Q method.

Table 3 lists the path attenuation coefficients, γ and Q_0, inverted with GLM, as well as the corresponding station magnitude corrections, $\Delta m_b(L_g)$, inverted with LSMF. Table 4 compares the resulting event $m_b(L_g)$ values with those by Nuttli's (1986b, 1987). Also included in Table 4 are *RMS* L_g magnitudes measured by Ringdal *et al.* (1992) using NORSAR and Grafenberg (GRF) recordings. Ringdal's L_g magnitudes are noise-corrected array averages, obtained by applying individual bias corrections for each array element.

Figure 2 shows the Q_0 values measured by Nuttli (1986b) based on the coda-*Q* method and those derived by our GLM scheme. Nuttli (1986b) initially estimated the path Q_0 with the coda-*Q* method of Aki and Chouet (1975) and Herrmann (1980), and then further refined his results with the simple network averaging of the station magnitudes. His initial and final Q_0 estimates are listed as $Q_0(1)$ and $Q_0(2)$, respectively, in Table 5. The GLM joint inversion gives a Q_0 of 756 for the Kazakh-COP path, which is 8% higher than Nuttli's value (Table 5). Thus events solely recorded at the station COP (such as Balapan explosion 850210) would

have significant discrepancy between Nuttli's original $m_b(L_g)$ and our GLM result. Nuttli did not find sufficient reliable data for the path from Eastern Kazakhstan to COP to determine the Q_0 and ζ with the coda-Q method, and hence the value for the station KON was used (Nuttli, 1986b; page 1243). These two stations are about 4300-4400 km away from the Eastern Kazakhstan test site with 7° difference in the azimuths. The station COP is right on the same direction as IRIS station OBN (Obninsk, Russia) for which Bennett *et al.* (1990) also find a Q_0 of 760.

COP recorded seven Balapan events: 801227, 820425, 820704, 840425, 840714, 841228, and 850210 (*viz.*, events marked with asterisk in Table 4). All these seven events have smaller GLM/LSMF $m_b(L_g)$ as compared to Nuttli's original network average. In particular, for Balapan event 850210 for which COP was the sole source of Nuttli's L_g recording, the GLM/LSMF $m_b(L_g)$ is identical to that of GRF and NORSAR, while Nuttli's $m_b(L_g)$ is 0.180 m.u. larger. This discrepancy of 0.180 m.u. happens to be the averaged station bias at COP derived with the LSMF inversion (Table 3). Event 850210 stands out in Figure 3 as an obvious outlier.

Take the Balapan event 841228 for another example, which Nuttli obtained station $m_b(L_g)$ values of 6.00 and 6.26 at stations NUR and COP, respectively. Subtracting the station terms of 0.004 and 0.180 would yield a simple network-averaged $m_b(L_g)$ of 6.038, which is closer to what Ringdal *et al.* (1992) measured. Balapan event 840425 is another event recorded at exactly the same two stations COP and NUR with station $m_b(L_g)$ of 5.85 and 5.87, respectively. With LSMF station corrections, the resulting event $m_b(L_g)$ is 5.768, which is, again, closer to the GRF $m_b(L_g)$. There is no GRF or NORSAR $m_b(L_g)$ of 820704 for comparison, and the remaining four events (801227, 820425, 840425, and 840714) were recorded at more stations, and hence the biasing effect at COP tends to be cancelled out somewhat by the network averaging. Nevertheless, applying the station corrections determined with LSMF or the path corrections determined with GLM systematically yields an event $m_b(L_g)$ closer to that determined with NORSAR and GRF data.

These 11 γ values shown in Table 3 have an average of 0.0021 km^{-1}. The 5 Scandinavian stations have an average γ of 0.0014 km^{-1}.

Both experiments are based on virtually equivalent linear models with the same data set as input. It is not surprising that both experiments would give the same standard deviation of ε of 0.108 magnitude unit, which is a measure of how well the model fits the data. In theory, this should imply that the uncertainty associated with the $m_b(L_g)$ of the same event should

remain identical under these two methods, even though the $m_b(L_g)$ itself could be varying due to different boundary conditions. However, the direct inversion result based on SVD is more sensitive the rounding error of the computer, and hence the resulting inverse matrix, $(\mathbf{H'H})^{-1}$, may not be as accurate as that obtained with the iterative inversion method. This is indicated by the slight deviation from the theoretically predicted uncertainty of $\sigma/\sqrt{\#(j)}$ in some of the LSMF-estimated standard errors in Table 4. Note that, however, both methods give almost identical event $m_b(L_g)$ values, even though two seemingly irrelevant boundary conditions were used. If, a more popular boundary condition that the 11 station terms have zero mean were used instead, then each station term (*viz.*, $\Delta m_b(L_g)$ in Table 3 or S(j) in Equation [4]) would be reduced by 0.016 m.u., and each LSMF $m_b(L_g)$ in Table 4 would then be increased by 0.016 m.u. accordingly. This will not affect our observation that the station residual at COP (now 0.164 m.u.) appears to be too large.

Table 3. GLM-inverted Coefficient of Anelastic Attenuation versus LSMF-inferred Station Corrections

Station				GLM Attenuation Coefficient		LSMF S(j)
Code	E°	N°	Paths	γ (1/km)	Q_0	$\Delta m_b(L_g)$
COP	12.433	55.683	7	0.00119	756	+0.180±0.051
KBL	69.043	34.541	15	0.00253	355	-0.028±0.040
KEV	27.007	69.755	11	0.00162	553	-0.116±0.037
KON	09.598	59.649	9	0.00126	713	+0.045±0.039
MHI	59.494	36.300	10	0.00240	374	-0.038±0.045
NDI	77.217	28.683	18	0.00295	305	+0.049±0.028
NIL	73.252	33.650	21	0.00244	367	-0.065±0.034
NUR	24.651	60.509	34	0.00154	581	+0.004±0.023
QUE	66.950	30.188	7	0.00296	303	+0.033±0.042
SHL	91.883	25.567	15	0.00257	349	+0.089±0.030
UME	20.237	63.815	10	0.00143	627	+0.026±0.036

Nuttli (1986)

GLM + Lg

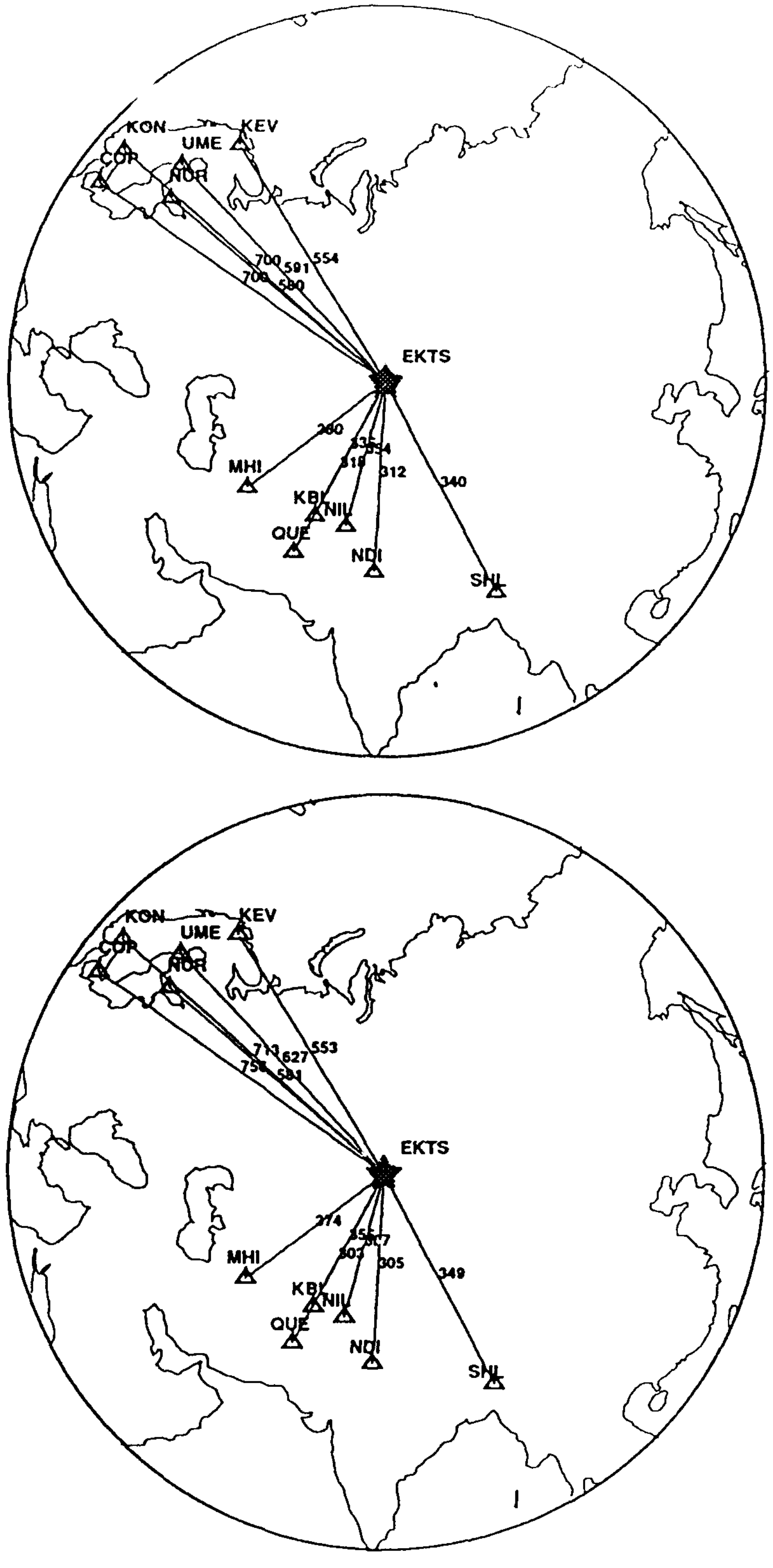

Figure 2. The Q_0 values measured by Nuttli (1986b) with the coda-Q method (top), and those derived by the GLM scheme (bottom). The GLM joint inversion gives a Q_0 of 756 for the Kazakh-COP path, which is 8% higher than Nuttli's guess. Thus events solely recorded at the station COP (such as Balapan explosion 02/10/85) would have significant discrepancy between Nuttli's original $m_b(L_g)$ and the GLM/LSMF result. Nuttli did not have sufficient reliable data for the path from Eastern Kazakhstan to COP to determine the Q_0 and ζ with the coda-Q method, and hence the values for the station KON were used (Nuttli, 1986b; page 1243). The station COP is right on the same azimuth as Russian IRIS stations OBN for which Bennett *et al.* (1990) also find a Q_0 of 760.

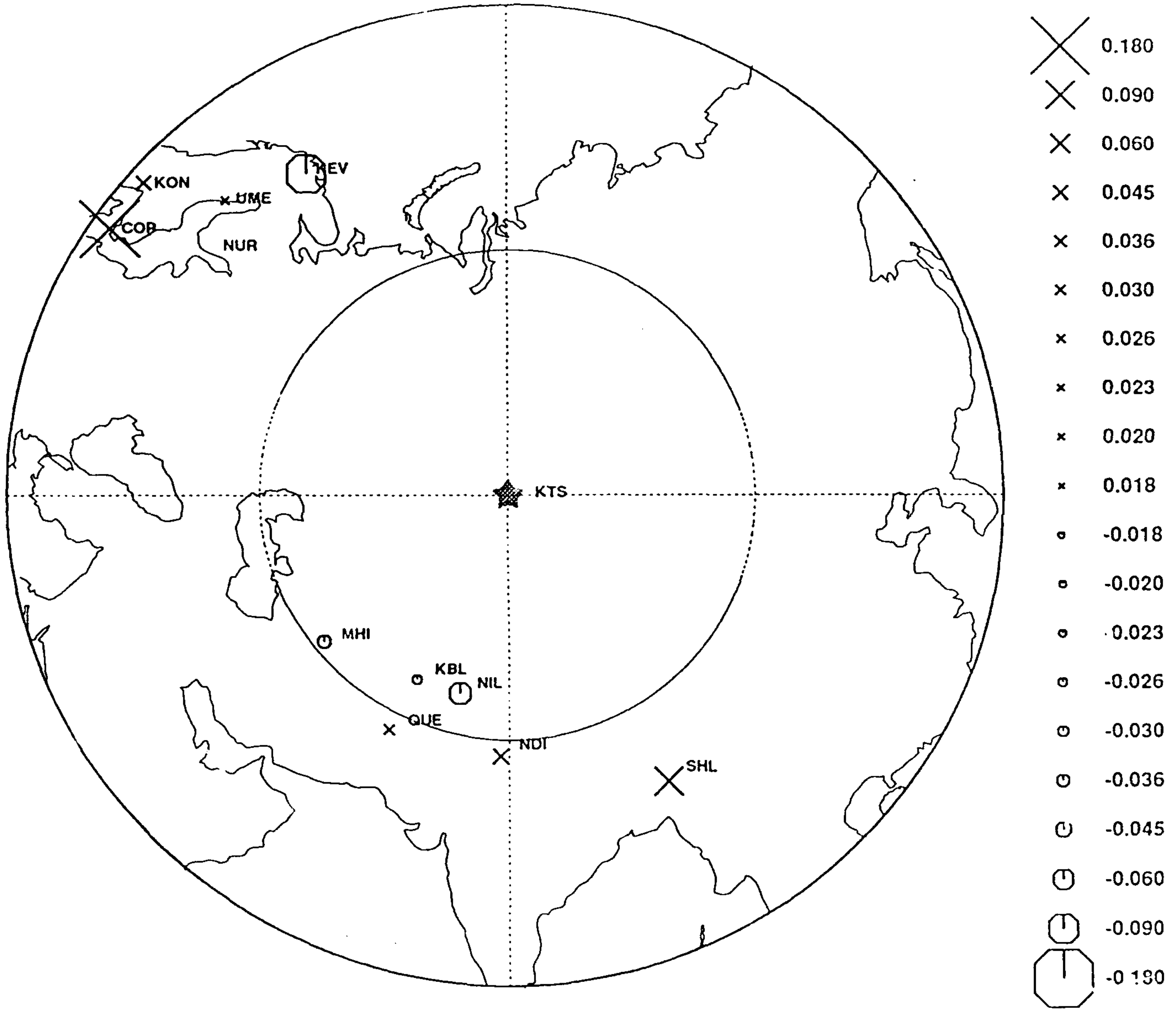

Figure 3. The $m_b(L_g)$ station terms derived with LSMF inversion. Nuttli (1986b, 1987) already included the attenuation correction in his $m_b(L_g)$ determination, therefore the station residuals (inferred by LSMF) should be relatively small for $m_b(L_g)$. The large positive station term at COP would suggest that Nuttli could have underestimated the path Q_0 for all paths from Eastern Kazakh to COP. The bias of 0.180 can be translated to an increase of 8% in the path Q_0, which would yield a Q_0 estimate identical to what obtained with the GLM iterative inversion method.

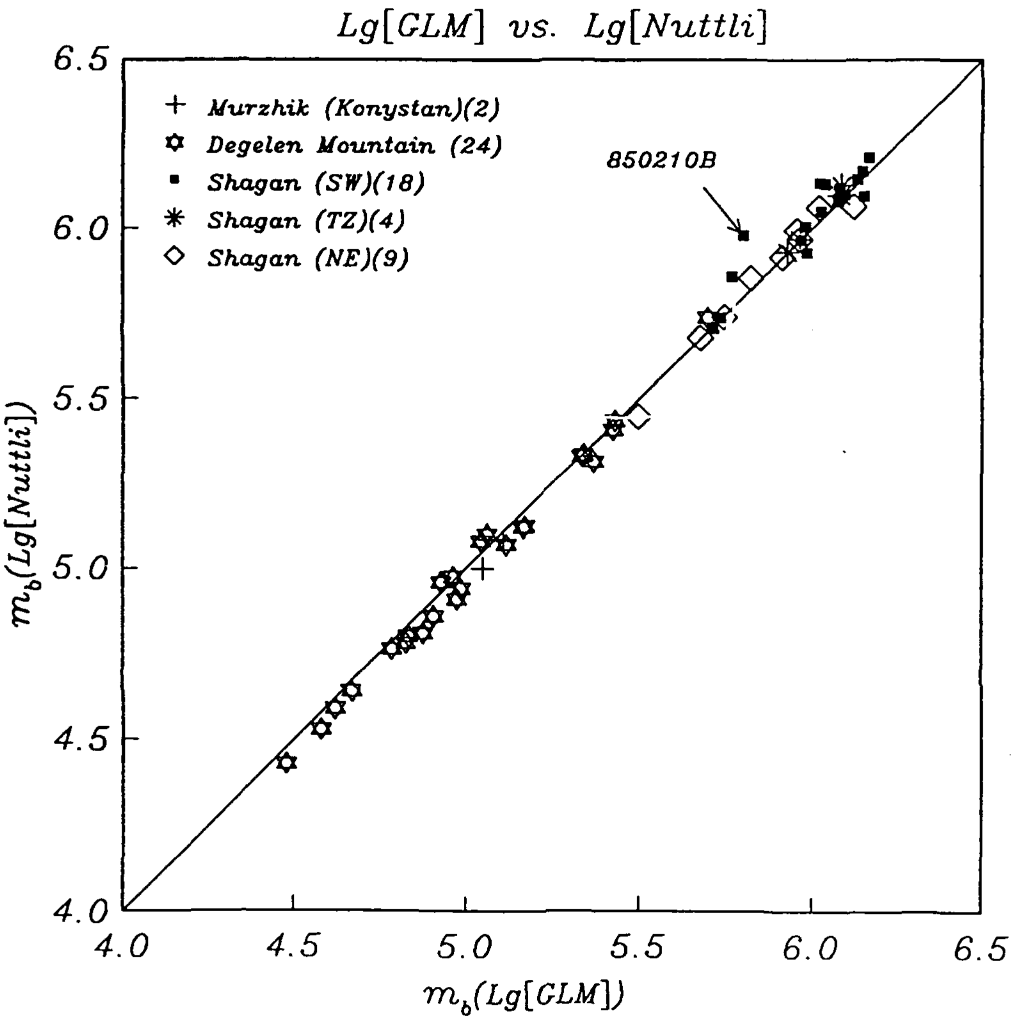

Figure 4. GLM/LSMF-reprocessed $m_b(L_g)$ values versus Nuttli's (1986b, 1987) $m_b(L_g)$ values. The Balapan event 02/10/85 stands out as an outlier. For all other 56 events, Nuttli's event $m_b(L_g)$ values appear to be very consistent with our reprocessed results.

Table 4. Comparison of Various $m_b(L_g)$					
Event	RMS L_g (Ringdal *et al.*, 1992)		Nuttli's $m_b(L_g)$	GLM $m_b(L_g)$	LSMF $m_b(L_g)$
Date	NORSAR	GRF	WWSSN	WWSSN	WWSSN
761123B	___	5.792	5.857±0.055 3	5.823±0.062	5.820±0.065
781129B	5.973	5.886	6.007±0.030 4	5.982±0.054	5.981±0.056
791028B	6.053	6.046	6.062±0.013 5	6.021±0.048	6.019±0.050
791202B	5.917	5.938	6.050±0.030 2	6.026±0.076	6.025±0.080
791223B	___	6.045	6.120±0.017 6	6.080±0.044	6.079±0.046
800612B	___	5.571	5.742±0.059 5	5.745±0.048	5.743±0.050
800629B	5.683	5.746	5.708±0.074 5	5.714±0.048	5.714±0.050
801012B	5.925	5.933	5.918±0.036 5	5.915±0.048	5.915±0.050
801214B	5.929	5.944	5.932±0.035 4	5.931±0.054	5.932±0.056
801227B *	5.939	5.885	5.996±0.038 7	5.959±0.041	5.958±0.042
810329B	5.556	5.437	5.450±0.100 2	5.498±0.076	5.497±0.083
810422B	5.908	5.956	5.968±0.025 4	5.969±0.054	5.968±0.056
810913B	6.113	6.106	6.098±0.065 6	6.083±0.044	6.082±0.046
811018B	5.985	5.956	6.088±0.066 5	6.075±0.048	6.074±0.050
811227B	6.074	6.092	6.146±0.067 5	6.133±0.048	6.132±0.050
820425B *	6.077	6.058	6.126±0.056 7	6.087±0.041	6.086±0.042
820704B *	___	___	6.135±0.015 2	6.023±0.076	6.022±0.083
821205B	5.990	6.002	6.210±0.090 2	6.165±0.076	6.163±0.079
831006B	5.870	5.843	5.930±0.070 2	5.986±0.076	5.986±0.080
831026B	6.000	6.036	6.100±___ 1	6.096±0.108	6.096±0.111
840219B	5.725	___	5.740±___ 1	5.735±0.108	5.736±0.111
840307B	5.698	5.575	5.680±___ 1	5.677±0.108	5.676±0.111
840329B	5.897	5.957	5.970±___ 1	5.965±0.108	5.966±0.111
840425B *	5.870	5.803	5.860±0.010 2	5.768±0.076	5.768±0.081
840526B	6.072	6.128	6.065±0.045 2	6.121±0.076	6.121±0.080
840714B *	6.054	6.064	6.170±0.208 3	6.148±0.062	6.147±0.066
841027B	6.085	6.145	6.095±0.055 2	6.151±0.076	6.151±0.080
841202B	5.880	5.860	5.970±___ 1	5.966±0.108	5.966±0.111
841216B	6.048	6.038	6.080±___ 1	6.076±0.108	6.076±0.111
841228B *	5.985	5.947	6.130±0.130 2	6.038±0.076	6.038±0.081
850210B *	5.803	5.801	5.980±___ 1	5.801±0.108	5.800±0.120

*: events recorded at COP.

Table 4. Comparison of Various $m_b(L_g)$					
Event	RMS L_g (Ringdal *et al.*, 1992)		Nuttli's $m_b(L_g)$	GLM $m_b(L_g)$	LSMF $m_b(L_g)$
Date	NORSAR	GRF	WWSSN	WWSSN	WWSSN
730710D	___	___	5.070±0.070 2	5.118±0.076	5.117±0.083
731026D	___	___	4.910±___ 1	4.975±0.108	4.975±0.113
740130bD	___	___	5.125±0.075 2	5.172±0.076	5.172±0.083
740516D	___	___	4.860±0.000 2	4.907±0.076	4.907±0.083
740710D	___	___	4.780±0.090 2	4.826±0.076	4.827±0.083
740913D	___	___	4.810±___ 1	4.876±0.108	4.875±0.113
741216aD	___	___	4.530±0.020 2	4.579±0.076	4.577±0.083
741216bD	___	___	4.430±0.050 2	4.477±0.076	4.477±0.083
750220D	___	___	5.410±0.058 3	5.424±0.062	5.425±0.066
750311D	___	___	5.315±0.055 2	5.366±0.076	5.367±0.082
750608D	___	___	5.100±___ 1	5.062±0.108	5.051±0.112
750807D	___	___	5.120±0.120 2	5.167±0.076	5.167±0.083
760115D	___	___	4.940±0.010 2	4.986±0.076	4.987±0.083
760421aD	___	___	4.960±0.020 2	4.929±0.076	4.933±0.079
760723D	___	___	4.640±___ 1	4.669±0.108	4.668±0.115
761230D	___	___	4.800±___ 1	4.834±0.108	4.838±0.117
770329D	___	___	5.335±0.018 4	5.338±0.054	5.338±0.056
770425D	___	___	4.975±0.085 2	4.964±0.076	4.969±0.081
770730D	___	___	4.763±0.054 3	4.785±0.062	4.784±0.065
771226D	___	___	4.590±___ 1	4.620±0.108	4.628±0.117
780326D	5.527**	___	5.436±0.069 5	5.429±0.048	5.428±0.050
780422D	5.141**	___	5.080±0.089 4	5.045±0.054	5.054±0.056
780728D	5.597**	___	5.330±0.023 3	5.333±0.062	5.333±0.065
781129D	___	___	5.740±0.046 4	5.698±0.054	5.698±0.056
730419M	___	___	5.080±0.020 2	5.111±0.076	5.111±0.079
780319M	___	___	5.000±0.050 2	5.050±0.076	5.052±0.082

**: from Ringdal (personal communication, 1991).

We can translate each LSMF station residual in Table 3 to a new estimate of the coefficient of anelastic attenuation with the following formula:

$$Q_0(\mathrm{new}) \approx \frac{1}{\dfrac{1}{Q_0(\mathrm{old})} - \dfrac{\Delta m_b(L_g)\cdot \ln(10)\cdot \mathrm{U}}{(\Delta - 10\mathrm{km})\cdot \pi}} \qquad [8]$$

This is essentially the same approach Nuttli (1986ab, 1987, 1988) and Patton (1988) used

previously. The resulting new Q_0 values are listed in Table 5 as $Q_0(4)$. Excellent agreement is obtained when comparing $Q_0(4)$ to those $Q_0(3)$ derived with GLM. Once again, this confirms that Q_0 for Kazakh-COP path should be higher than Nuttli's guess of 700. For other paths, however, Nuttli's original estimates based on the coda-Q method are generally rather consistent with our results based on the L_g -amplitude attenuation.

Table 5. Revised Q_0 for Semipalatinsk-WWSSN Paths

Station	Δ^*	Nuttli (1986b)			This Study	
Code	(km)	ζ	Q_0 (1)	Q_0 (2)	Q_0 (3)	Q_0 (4), $\Delta m_b(L_g)$
COP	4350	(0.4)	—	(700)	756	756, +0.180
KBL	1900	0.6	360	336	355	332, -0.028
KEV	3475	0.4	580	554	553	529, -0.116
KON	4375	0.4	700	700	713	713, +0.045
MHI	2150	0.5	380	380	374	374, -0.038
NDI	2375	0.6	300	312	305	317, +0.049
NIL	1875	0.6	380	354	367	343, -0.065
NUR	3525	0.4	580	580	581	581, +0.004
QUE	2425	0.6	300	318	303	322, +0.033
SHL	2925	0.6	300	340	349	349, +0.089
UME	3750	0.4	620	591	627	597, +0.026

*: rounded to the nearest 25 km (from Table 1 of Nuttli, 1986b).

**: Q_0: (1) Nuttli's initial measurement based on the coda-Q method; (2) Nuttli's refined Q_0 based on the single-event network averaging; (3) GLM result; (4) LSMF result.

6. DISCUSSION AND CONCLUSIONS

The GLM algorithm presented in this study can determine the path γ as well as the event $m_b(L_g)$ values simultaneously without the need to measure the path γ with other methods in advance. A staged LSMF inversion scheme has also been tested in this study. Both GLM and LSMF experiments yield very consistent results suggesting that the majority of Q_0 values Nuttli used in his pioneering L_g study of Semipalatinsk explosions (Nuttli, 1986b, 1987) are very good except for the path from Semipalatinsk to COP. Nuttli's biased attenuation correction at COP resulted in overestimated $m_b(L_g)$ for 7 Balapan events relative to the GLM/LSMF-recomputed event $m_b(L_g)$ values. In the extreme case, his $m_b(L_g)$ estimate for the Balapan event of 10 Feb 85 (which was determined solely based on the COP recording alone) is biased high by about 0.18 m.u. An 8% increase in the postulated coefficient of anelastic attenuation for this particular path is necessary. Other than this problem, Nuttli's (1986b, 1987) $m_b(L_g)$ data set for Semipalatinsk explosions has very good quality with a standard deviation (of single observation) of 0.1 m.u.

Our GLM algorithm is implemented with an iterative procedure instead of utilizing the standard matrix factorization or row elimination. The advantages of the iterative inversion scheme are obvious:

[1] It is rather easy to incorporate the boundary condition into the inversion scheme without altering the simple equations describing the underlying physical model. That is, the matrix elements of **H** will remain unchanged.

[2] The iterative scheme is numerically more accurate simply because it is less sensitive to rounding errors.

[3] When the number of equations becomes huge, the iterative method is often the only practical means to tackle the problem.

The only possible disadvantage is that the implementation of iterative methods usually depends on the actual application field. Therefore it may not be always easy to find a general-purpose linear-algebra library ready for use. On the other hand, packages suitable for direct methods are available in almost every commercial software library. However, this should not be considered as a serious drawback or limitation of the iterative method. Implementing the iterative procedure presented in this study is just as simple as coding up a program to call the standard linear algebra library.

The boundary condition used in our GLM experiment was that the resulting event $m_b(L_g)$ values would have the same mean as that of Nuttli's original $m_b(L_g)$ values. Magni-

tudes based on the short-period teleseismic recordings corrected for the station amplifications as well as the path effects (due to the focusing/defocusing near the source region *etc.*) such as those in Jih and Wagner (1992ab) may provide a good constraint as well. Many L_g studies have used the ISC m_b for "normalizing" their L_g magnitude scale (*e.g.*, page 2146 of Nuttli, 1986a; page 128 of Israelson, 1992).

If the test data all originated from the same test site, it would be very difficult to further decompose the path corrections into the station amplification (due to the local geology) and the propagation path effect. If, however, data from multiple test sites become available, then it is rather straightforward to adapt our GLM inversion model to a more general formulation which is almost identical to Equation [1] (as used in Jih and Wagner (1992ab)):

$$E(i) + S(j) - \gamma(k(i),j)(\Delta(i,j)-10\text{km})/\ln(10) + \varepsilon(i,j) = Y(i,j)\,, \qquad [3']$$

where k(i) represents the k-th test site where the i-th explosion is detonated.

Israelson (1992) applied the standard LSMF method to *RMS* L_g magnitudes measured on hand-digitized Soviet analog waveforms, and he obtained a suite of large station corrections ranging from -0.309 m.u. at NRI (Norilsk, Siberia) to 0.664 m.u. at UZH (Uzhgorod), on top of an assumed average γ of 0.0012km^{-1} for Russian Platform. Israelson (1992) finds that his station corrections seem to increase with the local ambient noise level at the receiver sites. There are other mechanisms that could reduce or enhance the L_g amplitude level, and yet they are not relevant to the local amplification. The blockage of Novaya Zemlya L_g as observed at KEV due to the thick sedimentary layer in Barents Sea is a good example (Baumgardt, 1991). Whatever mechanism it might actually be, for explosions confined in a small source region, either applying the extra bias corrections at the receivers (as did in Israelson, 1992; and in many m_b and M_S studies) or applying the path-wise γ correction (as did in the work of Nuttli, Patton, and many others) would serve equally well for the purpose of event magnitude determination. However, if the seismic events spread over a vast area so that they can no longer be grouped into just a few isolated test sites, then maintaining a tabular source-station path corrections may not be the most convenient approach. In such a case, a 2-dimensional map to describe the L_g Q variation would be necessary. The individual path γ values determined with GLM or the coda-Q method can and should be utilized to establish the 2-dimensional (*i.e.*, regionalized) Q map with the tomographic inversion. Establishing the regionalized Q map *in advance* with a suite of carefully measured events for seismotectonic regions of proliferation concern is particularly important, since there may not be sufficient data from the suspected clandestine tests for the coda Q determination (Jih and Lynnes, 1992).

7. ACKNOWLEDGEMENTS

The author wishes to thank DARPA/NMRO for recovering the station $m_b(L_g)$ values measured by Otto Nuttli. The PSLIB plotting library released by Paul Wessel (HIG) and Walter Smith (Scripps) has been used in preparing Figure 1. The geology shown in this figure was re-digitized by Abdul Malik based on a map of Bonham *et al.* (1980). Wilmer Rivers and Peter Davis reviewed and improved the original manuscript. This study was jointly supported under Phillips Laboratory contracts F19628-90-C-0158 and F29601-91-C-DB23. The views and conclusions contained in this paper are those of the author and should not be interpreted as representing the official policies, either expressed or implied, of Teledyne Inc., the U.S. Air Force, the Defense Advanced Research Projects Agency or the U.S. Government.

8. REFERENCES

Aki, K. and B. Chouet (1975). Origin of coda waves: source, attenuation, and scattering, *J. Geophys. Res.*, **80**, 3322-3342.

Baumgardt, D. R. (1991). High frequency array studies of long range L_g propagation and the causes of L_g blockage and attenuation in the Eurasian continental craton, *Report PL-TR-91-2059(I),* Phillips Laboratory, Hanscom Air Force Base, MA.

Bennett, T. J., J. F. Scheimer, A. K. Campanella, and J. R. Murphy (1990). Regional discrimination research and methodology implementation: analyses of CDSN and Soviet IRIS data, *Report GL-TR-90-0194,* Geophysics Laboratory, Hanscom Air Force Base, MA.

Blandford, R. R., and R. H. Shumway (1982). Magnitude:yield for nuclear explosions in granite at the Nevada Test Site and Algeria: joint determination with station effects and with data containing clipped and low-amplitude signals, *Report VSC-TR-82-12,* Teledyne Geotech, Alexandria, VA.

Bonham, S., W. J. Dempsey, J. Rachlin (1980). Geologic environment of the Semipalatinsk area, U.S.S.R. *(Preliminary Report),* U.S. Geological Survey, Reston, VA 22092.

Bunch, J. R. and D. J. Rose (eds.) (1976). *Sparse Matrix Computations,* Academic Press, New York, N.Y.

Douglas, A. (1966). A special purpose least squares programme, *AWRE Report No. O-54/66,* HMSO, London, UK.

Forsythe, G. E., M. A. Malcolm, and C. B. Moler (1977). *Computer Methods for Mathematical Computations,* Prentice Hall, Englewood Cliffs, NJ.

Golub, G. H. and C. F. Van Loan (1983). *Matrix Computations,* John Hopkins University

Press, Baltimore, MD.

Herrmann, R. B. (1980). Q estimates using the coda of local earthquakes, *Bull. Seism. Soc. Am.*, **70**, 447-468.

Israelson, H. (1992). RMS L_g as a yield estimator in Eurasia, *Report PL-TR-92-2217(I)*, Phillips Laboratory, Hanscom Air Force Base, MA.

Jih, R.-S. and C. S. Lynnes (1992). Re-examination of regional L_g Q variation in Iranian Plateau, in *Proceedings of 14th Annual PL/DARPA Seismic Research Symposium, 16-18 Sept 1992, Tucson, AZ.* (J. F. Lewkowicz and J. M. McPhetres (eds.)), *Report PL-TR-92-2210*, Phillips Laboratory, Hanscom Air Force Base, MA.

Jih, R.-S. and R. A. Wagner (1991). Recent methodological developments in magnitude determination and yield estimation with applications to Semipalatinsk explosions, *Report PL-TR-91-2212(I) (=TGAL-91-05)*, Phillips Laboratory, Hanscom Air Force Base, MA. **(ADA244503)**

Jih, R.-S. and R. A. Wagner (1992a). Path-corrected body-wave magnitudes and yield estimates of Novaya Zemlya explosions, *Report PL-TR-92-2042 (=TGAL-91-09)*, Phillips Laboratory, Hanscom Air Force Base, MA. **(ADA251240)**

Jih, R.-S. and R. A. Wagner (1992b). Path-corrected body-wave magnitudes and yield estimates of Semipalatinsk explosions, *Report TGAL-92-05*, Teledyne Geotech Alexandria Laboratory, Alexandria, VA.

Jih, R.-S. and R. H. Shumway (1989). Iterative network magnitude estimation and uncertainty assessment with noisy and clipped data, *Bull. Seism. Soc. Am.*, **79**, 1122-1141.

Lilwall, R. C. and Farthing, J. (1990). Joint epicentre determination of Soviet underground nuclear explosions 1973-89 at the Semipalatinsk Test Site, *AWE Report O-12/90*, HMSO, London, UK.

Marshall, P. D., T. C. Bache, and R. C. Lilwall (1984). Body-wave magnitudes and locations of Soviet underground explosions at the Semipalatinsk Test Site, *AWE Report O-16/84*, HMSO, London, UK.

Murphy, J. R., B. W. Barker, and A. O'Donnell (1989). Network-averaged teleseismic P-wave spectra for underground explosions. Part I - Definitions and Examples, *Bull. Seism. Soc. Am.*, **79-1**, 141-155.

Nuttli, O. W. (1986a). Yield estimates of Nevada Test Site explosions obtained from seismic L_g waves, *J. Geophys. Res.*, **91**, 2137-2151.

Nuttli, O. W. (1986b). L_g magnitudes of selected East Kazakhstan underground explosions, *Bull. Seism. Soc. Am.*, **76**, 1241-1251.

Nuttli, O. W. (1987). L_g magnitudes of Degelen, East Kazakhstan, underground explosions, *Bull. Seism. Soc. Am.*, **77**, 679-681.

Nuttli, O. W. (1988). L_g magnitudes and yield estimates for underground Novaya Zemlya nuclear explosions, *Bull. Seism. Soc. Am.*, **78**, 873-884.

Patton, H. J. (1988). Application of Nuttli's method to estimate yield of Nevada Test Site explosions recorded on Lawrence Livermore National Laboratory's digital seismic system, *Bull. Seism. Soc. Am.*, **78**, 1759-1772.

Press, W. H., B. P. Flannery, S. A. Teukolsky, and W. T. Vetterling (1988). *Numerical Recipes in C: the Art of Scientific Computing,* Cambridge University Press, Cambridge, UK.

Ringdal, F., P. D. Marshall, and R. Alewine (1992). Seismic yield determination of Soviet underground nuclear explosions at the Shagan River Test Site, *Geophys. J. Int.*, **109**, 65-77.

Spedicato, E. ed. (1991). *Computer Algorithm for Solving Linear Algebraic Equations: the State of the Art, NATO ASI Series,* Springer-Verlag, Berlin, Germany.

Tewarson, R. P. (1973). *Sparse Matrices,* Academic Press, New York, NY.

DISTRIBUTION LIST

NON-GOVERNMENT CONTRACTORS

Prof. Thomas Ahrens
Seismological Lab, 252-21
Div. of Geol. & Planetary Sciences
California Institute of Technology
Pasadena, CA 91125

Dr. Thomas C. Bache, Jr.
Dr. Thomas J. Sereno, Jr.
Science Applications Int'l Corp.
10260 Campus Point Drive
San Diego, CA 92121 (2)

Dr. Peter Basham
Dr. Robert North
Earth Physics Branch
Geological Survey of Canada
1 Observatory Crescent
Ottawa, Ontario,CANADA K1A OY3

Dr. Douglas R. Baumgardt
Dr. Zoltan A. Der
ENSCO, Inc.
5400 Port Royal Road
Springfield, VA 22151-2388

Prof. Jonathan Berger
IGPP, A-025
Scripps Institution of Oceanography
University of California, San Diego
La Jolla, CA 92093

Dr. G. A. Bollinger
Department of Geological Sciences
Virginia Polytechnic Institute
21044 Derring Hall
Blacksburg, VA 24061

The Librarian
Dr. Jerry Carter
Dr. Stephen Bratt
Center for Seismic Studies
1300 North 17th Street, Suite 1450
Arlington, VA 22209-2308 (3)

Michael Browne
Teledyne Geotech
3401 Shiloh Road
Garland, TX 75041

Dr. Lawrence J. Burdick
Woodward-Clyde Consultants
566 El Dorado Street
Pasadena, CA 91109-3245

Dr. Theodore Cherry
Science Horizons, Inc.
710 Encinitas Blvd, Suite 200
Encinitas, CA 92024 (2)

Dr. Kin-Yip Chun
Geophysics Division
Physics Department
University of Toronto
Ontario, CANADA M5S IA7

Dr. Paul M. Davis
Dept. Earth & Space Sciences
University of California (UCLA)
Los Angeles, CA 90024

Prof. Steven Day
Department of Geological Sciences
San Diego State University
San Diego, CA 92182

Ms. Eva Johannisson
Senior Research Officer
National Defense Research Institute
P.O. Box 27322
S-102 54 Stockholm, SWEDEN

Dr. Mark D. Fisk
Mission Research Corporation
735 State Street
P.O. Drawer 719
Santa Barbara, CA 93102

Prof. Stanley Flatte
Applied Sciences Building
University of California
Santa Cruz, CA 95064

Dr. Roger Fritzel
Pacific Sierra Research
1401 Wilson Blvd., Suite 1100
Arlington, VA 22209

Dr. Holly K. Given
Inst. Geophys. & Planet. Phys.
Scripps Inst. Oceanography (A-025)
University of California, San Diego
La Jolla, CA 92093

Prof. Hans-Peter Harjes
Institute for Geophysik
Ruhr University/Bochum
P.O. Box 102148
463 Bochum 1, FRG

Prof. Donald V. Helmberger
Seismological Laboratory
Div. of Geol. & Planetary Sciences
California Institute of Technology
Pasadena, CA 91125

Prof. Eugene Herrin
Prof. Brian Stump
Inst. for the Study of Earth and Man
Geophysical Laboratory
Southern Methodist University
Dallas, TX 75275

Prof. Bryan Isacks
Prof. Muawia Barazangi
Cornell University
Department of Geological Sciences
SNEE Hall
Ithaca, NY 14850

Prof. Lane R. Johnson
Prof. Thomas V. McEvilly
Seismographic Station
University of California
Berkeley, CA 94720

Robert C. Kemerait
ENSCO, Inc.
445 Pineda Court
Melbourne, FL 32940

Prof. Brian L.N. Kennett
Research School of Earth Sciences
Institute of Advanced Studies
G.P.O. Box 4
Canberra 2601, AUSTRALIA

Dr. Richard LaCoss
MIT-Lincoln Laboratory
M-200B
P.O. Box 73
Lexington, MA 02173-0073

Prof. Fred K. Lamb
Univ. of Illinois
Department of Physics
1110 West Green Street
Urbana, IL 61801

Prof. Charles A. Langston
Geosciences Department
403 Deike Building
The Pennsylvania State University
University Park, PA 16802

Prof. Thorne Lay
Dr. Susan Schwartz
Institute of Tectonics
Earth Science Board
University of California, Santa Cruz
Santa Cruz, CA 95064

Prof. Arthur Lerner-Lam
Prof. Paul Richards
Prof. C.H. Scholz
Lamont-Doherty Geol. Observatory
of Columbia University
Palisades, NY 10964

Dr. Manfred Henger
Fed. Inst. for Geosci. & Nat'l Res.
Postfach 510153
D-3000 Hanover 51, FRG

Dr. Peter Marshall
Dr. Alan Douglas
Procurement Executive
Ministry of Defense
Blacknest, Brimpton
Reading FG7-4RS, United Kingdom

Dr. Randolph Martin, III
New England Research , Inc.
76 Olcott Drive
White River Junction, VT 05001

Dr. Bernard Massinon
Societe Radiomana
27 rue Claude Bernard
75005 Paris, FRANCE (2)

Dr. Gary McCartor
Prof. Henry L. Gray
Department of Physics
Southern Methodist University
Dallas, TX 75275

Dr. Keith L. McLaughlin
S-Cubed
P.O. Box 1620
La Jolla, CA 92038-1620

Dr. Pierre Mecheler
Societe Radioman
27 rue Claude Bernard
75005 Paris, FRANCE

Prof. Bernard Minster
Prof. John Orcutt
IGPP, A-025
Scripps Institute of Oceanography
University of California, San Diego
La Jolla, CA 92093

Prof. Brian J. Mitchell
Dr. Robert Herrmann
Dept. of Earth & Atmospheric Sciences
St. Louis University
St. Louis, MO 63156

Mr. Jack Murphy
S-Cubed
11800 Sunrise Valley Drive
Suite 1212
Reston, VA 22091 (2)

Dr. Jay J. Pulli
Radix Systems, Inc.
2 Taft Court, Suite 203
Rockville, MD 20850

Dr. Frode Ringdal
Dr. Svein Mykkeltveit
NTNF/NORSAR
P.O. Box 51
N-2007 Kjeller, NORWAY (2)

Mr. Wilmer Rivers, Jr.
Teledyne Geotech Alexandria Laboratory
314 Montgomery Street
Alexandria, VA 22314-1581

Dr. Richard Sailor
TASC, Inc.
55 Walkers Brook Drive
Reading, MA 01867

Prof. Charles G. Sammis
Prof. Kei Aki
Center for Earth Sciences
University of Southern California
University Park
Los Angeles, CA 90089-0741

Prof. David G. Simpson
Lamont-Doherty Geological Observatory
of Columbia University
Palisades, NY 10964

Dr. Stewart W. Smith
Geophysics AK-50
University of Washington
Seattle, WA 98195

Prof. Clifford Thurber
Prof. Robert P. Meyer
University of Wisconsin-Madison
Department of Geology & Geophysics
1215 West Dayton Street
Madison, WS 53706

Prof. M. Nafi Toksoz
Earth Resources Lab
Mass. Institute of Technology
42 Carleton Street
Cambridge, MA 02142

Prof. Terry C. Wallace
Dept. of Geosciences
Building #77
University of Arizona
Tucson, AZ 85721

Dr. William Wortman
Mission Research Corporation
735 State Street
P.O. Drawer 719
Santa Barbara,CA 93102

U.S. GOVERNMENT AGENCIES

Mr. Alfred Lieberman
ACDA/VI-OA, Room 5726
320 21st Street, N.W.
Washington, D.C. 20451

Colonel Jerry J. Perrizo
AFOSR/NP, Building 410
Bolling AFB
Washington, D.C. 20331-6448

Dr. Robert R. Blandford
AFTAC/CSS
1300 N. 17th Street, Suite 1450
Arlington, VA 22209

AFTAC/CA
(STINFO)
Patrick AFB, FL 32925-6001

Dr. Frank F. Pilotte
HQ AFTAC/TT
Patrick AFB, FL 32925-6001

Katie Poley
CIA-ACIS/TMC
Room 4X16NHB
Washington, D.C. 20505

Dr. Larry Turnbull
CIA-OSWR/NED
Washington, DC 20505

Dr. Ralph W. Alewine, III
Dr. Alan S. Ryall, Jr.
DARPA/NMRO
3701 N. Fairfax Drive
Arlington, VA 22303-1714 (7)

DARPA/OASB/Librarian
3701 N. Fairfax Drive
Arlington, VA 22303-1714

Dr. Dale Glover
DIA/DT-1B
Washington, D.C. 20301

Dr. Michael Shore
Defense Nuclear Agency/SPSS
6801 Telegraph Road
Alexandria, VA 22310

Dr. Max Koontz
U.S. Dept. of Energy/DP-5
Forrestal Building
1000 Independence Avenue
Washington, D.C. 20585

Defense Technical Information Center
Cameron Station
Alexandria, VA 22314 (2)

Dr. John J. Cipar, PL/GPEH
Dr. Anton W. Dainty
Phillips Lab/Geophysics Directorate
Hanscom AFB, MA 01731 (2)

James F. Lewkowicz, PL/GPEH
Phillips Lab/Geophysics Directorate
Hanscom AFB, MA 01731

Phillips Laboratory (PL/XO)
Hanscom AFB, MA 01731

Dr. James Hannon
Lawrence Livermore National Laboratory
P.O. Box 808
Livermore, Ca 94550 (2)

Office of the Secretary of Defense
DDR&E
Washington, D.C. 20330

Eric Chael
Division 9241
Sandia Laboratory
Albuquerque, NM 87185

Dr. William Leith
U.S. Geological Survey
Mail Stop 928
Reston, VA 22092

Dr. Robert Masse
Box 25046, Mail Stop 967
Denver Federal Center
Denver, CO 80225

Dr. Robert Reinke
WL/NTESG
Kirtland, AFB, NM 87117-6008

(THIS PAGE INTENTIONALLY LEFT BLANK)